

Open Access Article

## Properties of Locally-Sourced Rice Husk Ash (RHA)-Blended Mortar

Chinh Van Nguyen

Faculty of Civil Engineering, The University of Danang - University of Science and Technology, Danang, Vietnam

**Abstract:** The present study is aimed to investigate the effects of different proportions of locally sourced RHA in Vietnam on the mechanical properties, microstructure and porosity of cement mortar. RHA is a material that was used to replace the original Portland cement (OPC). Prisms of dimensions of 40x40x160mm were cast and cured in water to determine the flexural and compressive strengths at 7 days and 28 days. The porosity was studied by Mercury Intrusion Porosimetry (MIP), while the microstructure of RHA mortar was determined by Scanning Electron Microscope (SEM). The results show that RHA reduces the workability of fresh mortar unless water reducing admixture is added, due to the porosity of RHA leading to an increase in the surface area of RHA. The locally-sourced RHA reduces the strengths at 7 and 28 days; however, the strength improves with age due to the latent pozzolanic reaction between RHA and  $\text{Ca}(\text{OH})_2$ . In addition, 5% and 20% RHA both increase the effective porosity and cumulative intruded volume, while 10% RHA reduces those properties at both 7 days and 28 days.

**Keywords:** mortar, rice husk ash, strength, microstructure, porosity.

### 本地混合的稻壳灰 (RHA) 砂浆的性能

**摘要:** 本研究旨在调查越南不同比例的RHA对水泥砂浆的力学性能, 微观结构和孔隙率的影响。RHA是用于替代原始波特兰水泥 (OPC) 的材料。在水中浇筑并固化尺寸为40x40x160毫米的棱镜, 以确定在7天和28天时的抗弯强度和抗压强度。用水银压入孔率法 (MIP) 研究孔隙度, 用扫描电子显微镜 (扫描电镜) 测定RHA砂浆的微观结构。结果表明, 除非添加减水剂, 否则RHA会降低新鲜砂浆的可加工性, 这是由于RHA的孔隙率导致RHA表面积增加。本地采购的RHA会在7天和28天时降低强度。但是, 由于RHA和钙 (哦)  $2$  之间潜在的火山灰反应, 强度会随着年龄的增长而提高。此外, 5%和20%的RHA均会增加有效孔隙率和累积侵入体积, 而10%的RHA会在7天和28天同时降低这些性能。

**关键词:** 砂浆, 稻壳灰, 强度, 微结构, 孔隙率。

## 1. Introduction

Mortar is an effective paste consisting of cement, sand, and water. It is used to bind different types of building blocks, such as stone, bricks, and concrete masonry by sealing the regular/irregular openings between them [50]. The most common binders used in mortar are Portland cement and lime [1]. Mortar used in construction needs to meet the relevant requirements in the consistency of fresh mortar and the strength of

hardened mortar in accordance with standard TCVN 4314: 2003 [2].

Nowadays, given the drive toward sustainable development practices in the construction industry, researchers have conducted a wide range of studies on the utilization of waste materials as supplementary cementitious materials. The common pozzolanic agents deriving from industry and agriculture by-products, such as fly ash and rice husk ash (RHA), are being

Received: 16 February 2021 / Revised: 13 March 2021 / Accepted: 17 March 2021 / Published: 30 April 2021

Fund Project: The University of Danang - University of Science and Technology (Code number of Project: T2020-02-28)

About the author: Chinh Van Nguyen, Ph.D., Faculty of Civil Engineering, The University of Danang - University of Science and Technology, Danang, Vietnam

Corresponding author Chinh Van Nguyen, [nvchinh@dut.udn.vn](mailto:nvchinh@dut.udn.vn)

studied as they diversify the product quality of the blended cement concrete and reduce the cost and negative environmental impact [3, 4]. Fly ash is a by-product of the combustion of pulverized coal in thermal power plants. It has been used as a supplementary cementitious material (SCM) to replace Portland cement in mortar and concrete [5, 6] and is recognized in the standards covering SCMs [7, 8]. The economic and performance advantages of using fly ash as a supplementary cementitious material include saving the resources used in the production of Portland cement, improved workability, enhanced mix efficiency and increased durability, and corrosion resistance [9, 10]. More recently, the focus for the use of fly ash in concrete has shifted to quantifying the benefits offered in enhancing concrete sustainability [11]. However, there are also several drawbacks to using fly ash in concrete, which include the extended setting time, reduced early age strengths, and reduced carbonation resistance [6].

Rice husk is one of the main agricultural residues obtained from the outer covering of rice grains during the milling process. It constitutes 20% of the 500 million tons of paddy produced in the world [12]. Rice husk ash, which had previously been dumped into water streams and caused the pollution and contamination of springs, is considered a useful mineral admixture for concrete [13, 14, 49]. Rice husk is abundant in many parts of the world, especially in rice-cropping countries like Vietnam. Each ton of paddy rice can produce approximately 200 kg of rice husk, which, on combustion, produces about 40 kg of ash [15]. According to the "Rice market monitor" report [16], in 2017, global rice paddy production was about 759.6 million tons (in which the Vietnam paddy production was about 42 million tons), resulting in approximately 145 million tons of rice husks. RHA is the residue of completely incinerated rice husk under proper conditions. The most important characteristic of RHA is pore structure, which affects the specific surface area, pozzolanic reactivity, and water absorption of RHA [10, 15, 17]. The rice husk ash properties depend upon incinerating conditions, rate of heating, geographic location, and fineness [18, 19].

Previous research shows that RHA can fully substitute silica fume in terms of calcium hydroxide consumption, autogenous shrinkage, compressive strength, and the durability of high performance concrete [15, 20] and ultra-high performance concrete [17, 21]. Some research shows that RHA reduced the strength of mortar or concrete. For example, the addition of up to 15% RHA from Thailand contributes to a reduction of more than 40% in the compressive strength of mortar at 24 days due to the increase in porosity. In addition, the carbon and impurity in RHA contributed to a further reduction in compressive strength [22]. Dabai et al. pointed out that the compressive strength of mortar at 28 days reduced

when RHA proportions increased, as well as a reduction of 27% when the mortar was blended with 20% of RHA (by weight of cement) [23]. By contrast, other research shows that RHA increases the compressive strength of mortar or concrete [24, 25]. The compressive strength of RHA-blended concrete or mortar depends upon the water to cement ratio, curing condition, RHA replacement level, and type/source of RHA, including the particle size [26].

Porosity of cement-based material is a key parameter affecting strength, permeability, and durability. The pore structure of cement-based materials includes air voids, capillary pores, and gel pores [27, 28]. Different techniques are used to determine the pore structures of mortar, in which mercury intrusion porosimetry (MIP) is an available method to determine the pore size distribution. MIP can determine the mean pore diameter, threshold radius, and total porosity, which are the most crucial parameters describing pore size distribution [27]. The porosity of cement paste depends on many factors and typically decreases with the water to cement ratio and age [29]. In addition, the type of cement/binder also affects porosity [30]. Therefore, replacing OPC with supplementary cementitious materials will influence the porosity of mortar.

The present study aimed to investigate the effect of different proportions of locally-sourced RHA in Vietnam used to replace the original Portland cement (OPC) on the mechanical properties, microstructure, and porosity of cement mortar. RHA was used to replace OPC at three proportions: 5%, 10%, and 20% by weight, respectively. Porosity was studied using MIP, while the microstructure of RHA mortar was studied by SEM. The successful incorporation of RHA into mortar brings a positive impact to the environment as it helps to sort out the rice husk, which was usually burned in the field. In addition, it also helps to reduce the Portland cement used in construction, which also leads to a reduction in CO<sub>2</sub> emissions.

## 2. Materials and Methods

### 2.1. Materials

The OPC, supplied by Song Gianh Ltd, Vietnam, met the requirements of TCVN 2682:2009 [31]. The fine aggregate was natural sand from the Ky Lam River, Quang Nam, Vietnam, and met the requirements of TCVN 1770: 1996 [32]. Rice husk ash (RHA) was obtained from MTX Ltd in Binh Phuoc, Vietnam. The chemical composition of RHA is presented in Table 1. X-ray powder diffraction (XRD) of RHA (Fig. 1) was obtained through the use of a Philips X-1 Pert X-ray diffractometer. XRD was operated with a Cu K $\alpha$  radiation source (40 KV and 40 mA, wavelength  $\lambda=1.5406\text{nm}$  [6.07 x10<sup>-9</sup> 2 in.]) by scanning from 5° to 75° at an angle of 2 $\theta$ . The scan step size is 0.0131303.

X-ray data were fitted using the pseudo-Voigt profile function and refined by means of Rietveld.

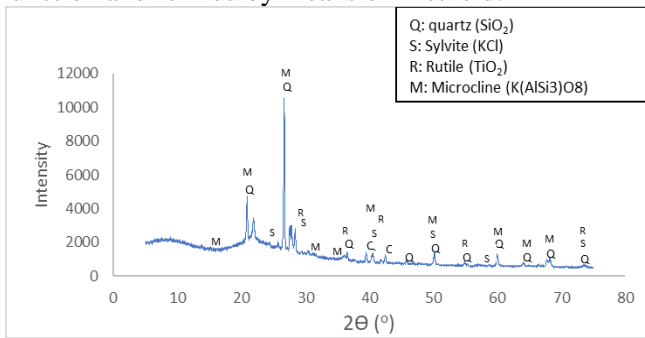


Fig. 1 X-ray diffraction patterns of RHA

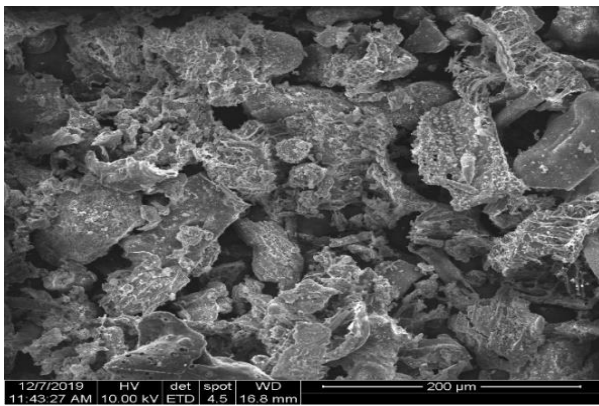


Fig. 2 SEM image of RHA

Fig. 1 shows peaks for quartz, microcline, rutile and sylvite. The highest peak is quartz, representing the crystalline phase of the silica content, which is attributed to the high temperature of the burning process of RHA. The Scanning Electron Microscope (SEM) image of RHA was obtained by using the QUANTA 650, and is presented in Fig. 2. A water-reducing admixture, Sikamen R4, was supplied by the Sika group meeting the requirements of ASTM C494 [33].

Table 1 Chemical composition of Portland cement and RHA

Constituents	RHA	OPC
MgO %	0.864	0.982
Al <sub>2</sub> O <sub>3</sub> %	1.999	5.513
SiO <sub>2</sub> %	84.296	18.311
SO <sub>3</sub> %	0.144	2.544
K <sub>2</sub> O %	6.961	1.005
CaO %	2.334	68.621
TiO <sub>2</sub> %	0.184	0.11
MnO %	0.152	-
Fe <sub>2</sub> O <sub>3</sub> %	1.321	2.612
SrO %	-	0.042
P <sub>2</sub> O <sub>5</sub> %	0.737	0.064
ZnO %	-	0.08
Cl %	1.009	0.117

## 2.2. Mix Proportions and Samples Preparation

Details of mix proportions are shown in Table 2. The mortar proportions for binder, sand and water were 1.0:2.0:0.5, in which the binder consists of a mixture of OPC and RHA. RHA was used to replace OPC at the proportions of 5%, 10% and 20% by weight, respectively. The mix proportion was selected to

achieve the mortar grade of M20 in accordance with TCVN 4314:2003 [2]. The negative effect of incorporation of RHA into mortar or concrete is a reduction in workability, as it increases the surface area of binder. The larger the specific surface area of the component, the greater its water demand [34, 35]. Therefore, water reducing admixture was used to ensure a flow of fresh mortar of approximately 20 cm, meeting the consistency requirement for fresh mortar in accordance with TCVN 4314:2003 [2]. Samples of 40x40x160 mm were cast and demoulded after 24 hours. After demoulding, prisms were cured in the water until test dates of 7 and 28 days.

Table 2 Details of mix proportions

ID	OPC	RHA	Sand	WRA	W/B	Flow (cm)
M0	1	0	2	0%	0.5	20.5
M1	0.95	0.05	2	0.50%	0.5	22.0
M2	0.9	0.1	2	1%	0.5	20.5
M3	0.8	0.2	2	2.5%	0.5	18.0

Notes:

+WRA = water-reducing admixture (by weight of binder)

+W/B = water to binder ratio

+B = binder, which consists of OPC and RHA

## 2.3. Test Procedure

### 2.3.1. Consistency of Fresh Mortar

The workability of fresh mortar was measured using the flow table test, in accordance with TCVN 3121-3:2003 [36]. The flow value represented the mean diameter of a test sample of the fresh mortar placed on the flow table disc by means of a defined mould, and given a number of vertical impacts by raising the flow table and allowing it to fall freely from a given height.

### 2.3.2. Mechanical Properties

The flexural and compressive strengths were determined in accordance with TCVN 3121-11:2003 [37]. The three-point bending test method was used to determine the flexural strength. The two halves of the broken prisms from the flexural strength tests were used to determine the compressive strength. The strength measurements of mortar were made at 7 and 28 day age. Each result of the flexural and compressive strength was the average value of three and six specimens, respectively.

### 2.3.3. Scanning Electron Microscope (SEM)

SEM (QUANTA 650) was used to observe the cementitious matrix. Samples for SEM were taken from the 7 and 28 days age specimens, respectively, oven-dried for 4 hours before coating with a 20 nm thick layer of gold using a Quorum Q150T. SEM images were obtained with an ETD detector, a working distance of about 10 mm, an accelerating voltage of 5 kV, and a spot size of 4 nm.

### 2.3.4. Mercury Intrusion Porosimetry (MIP)

The effect of RHA on the porosity and pore size distribution of mortar was determined by mercury intrusion porosimetry using the PASCAL 140/240. Porosimeter samples were obtained from the inner core of 40x40x160mm prisms used for flexural strength tests. The weight of the MIP samples was between 1 - 2g (0.002 - 0.004 lb) with an average length of 1 cm (0.39 in.). The MIP samples were placed in an oven (50°C) for three days to remove water presented within the pores of its matrix. The oven-dried samples were then immersed in acetone for 4 h before placing them inside a desiccator for a minimum of 24 h until they were tested. The desiccator has silica gel at its bottom to prevent moisture migration from the air. The diameter of pores was calculated according to the Washburn equation given below:

$$P=2\gamma\cos\theta/r \quad (1)$$

where P is the applied pressure (Pa); r is the radius of pores (nm);  $\gamma$  is the surface tension of mercury (N m<sup>-1</sup>);  $\theta$  is the contact angle between mercury and concrete (assumed as 140). The surface tension of mercury is 0.48 N m<sup>-1</sup>.

### 3. Results and Discussion

#### 3.1. Workability

The flows of all mixes are given in Table 1. RHA reduced the flow and was compensated by the water-reducing admixtures, so the flow of all four mixes was kept at around 20 cm. This ensures that it can be cast easily. This agrees well with the previous research where RHA reduced the workability unless water-reducing admixtures were used. RHA influenced greatly the normal consistency of the cement paste mixture, blended up to 20% by weight of Portland cement, as RHA absorbs large amounts of water [34]. Other research also concluded that blending RHA into a concrete mix leads to an increased amount of water, and a superplasticiser was used to obtain the targeted workability of the fresh concrete. RHA blended concrete requires more water for a given consistency due to its adsorptive character of cellular RHA particles and its high fineness, which leads to an increase in its specific surface area [35]. Research also shows that the superplasticiser content increases when the RHA proportions increase [38]. The higher water required when RHA is added to the mixes can be explained by the fact that RHA is a porous material with macro- and meso-pores inside and on the surface of the particles, making a very large specific surface area. RHA absorbed a certain amount of water on its surface, reducing the free water and producing less workability [26].

#### 3.2. Compressive Strength

The compressive strength of all the mortar mixes is shown in Fig. 3. The ratio of the compressive strength of the RHA mortar to the control mix is also presented

in Fig. 3. It can be seen that RHA reduces the compressive strength of mortar at both 7 days and 28 days; the more the proportion of RHA, the greater the reduction in the compressive strength. At 7 days the compressive strength of the control sample is 21.18 MPa while it is 17.58 MPa, 13.61 MPa, and 6.39 MPa for M1 (5% RHA), M2 (10% RHA), and M3 (20% RHA), respectively. This is equivalent to 0.83, 0.64, and 0.3, respectively, for the compressive strength of the control sample (M0). At 28 days the compressive strength of the control sample is 29.16 MPa while it is 26.86 MPa, 19.99 MPa, and 11.99 MPa for M1 (5% RHA), M2 (10% RHA), and M3 (20% RHA), respectively. This is equivalent to 0.92, 0.69, and 0.41, respectively, for the compressive strength of the control sample (M0). This agrees well with some previous research where RHA reduced the compressive strength of mortar or concrete [22, 23, 38].

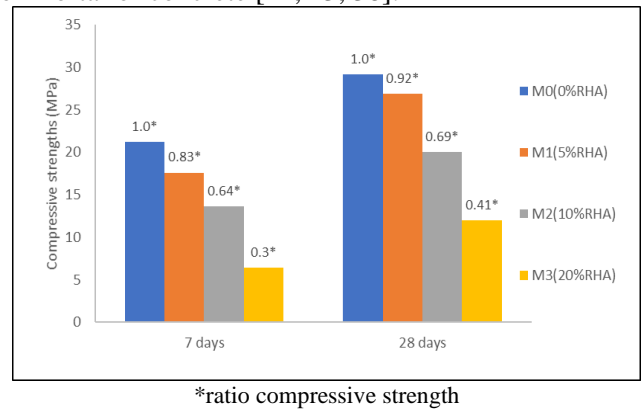


Fig. 3 Compressive strength of control and RHA blended cement mortars at 7 and 28 days

Fig. 3 also shows that the ratio of compressive strength of RHA samples to the control samples is increased with the increase of curing time, predicting that the compressive strength of RHA samples is higher than that of the control samples at a later age. The ratios increase from 0.83 at seven days to 0.92 at 28 days for M1 (5%RHA), from 0.64 at seven days to 0.69 at 28 days for M2 (10%RHA), from 0.3 at seven days to 0.41 at 28 days for M3 (20%RHA). Therefore, it is predicted that the ratio of compressive strength of 5% RHA samples will be greater than 1.0 at later than 28 days. This agrees well with previous research, where at an early age, the amount of up to 20%RHA reduced the OPC in the mix and increased the volume of capillary pores leading to the accumulating CH on the interface. This causes a lower strength than that of the control specimens without RHA. However, at a later age (normally after 28 days), the compressive strength is enhanced as the pozzolanic reaction starts, decreasing CH and increasing the densification [38].

The reduction in the compressive strength of the RHA samples compared with the control sample can be explained by the late pozzolanic reaction of the RHA and Ca(OH)<sub>2</sub> [26]. Pozzolanic properties refer to the chemical reaction between RHA, calcium hydroxide, and water; this reaction plays an important role in



determining concrete strength. In RHA, pozzolanic activity is delayed due to the larger particle sizes and higher carbon content of RHA compared with the silica fume [26]. This pozzolanic delay can further be explained by the cellular porous structure of RHA particles—the silica inside the RHA particles must first diffuse to the surface of these particles and then diffuse to the solution in order to combine with calcium hydroxide [17].

### 3.3. Flexural Strength

The flexural strengths of the mortar mixes are shown in Fig. 4. The ratio of the flexural strength of the RHA mortar to the control mix is also presented in Fig. 4. It is clear that the RHA reduced the flexural strength of the mortar at both 7 days and 28 days—the greater the proportion of RHA, the greater the reduction in flexural strength. At 7 days, the flexural strength of the control sample was 5.71 MPa, whereas it was 4.14 MPa, 3.5 MPa, and 3.22 MPa for M1 (5% RHA), M2 (10% RHA), and M3 (20% RHA), respectively. The ratios of flexural strength of M1 (5% RHA), M2 (10% RHA), and M3 (20% RHA) to the control sample (M0) are 0.73, 0.61, and 0.57, respectively. At 28 days, the flexural strength of the control sample was 6.66 MPa, whereas it was 6.08 MPa, 4.96 MPa, and 4.22 MPa for M1 (5% RHA), M2 (10% RHA), and M3 (20% RHA), respectively. The ratios of flexural strength of M1 (5% RHA), M2 (10% RHA), and M3 (20% RHA) to the control sample (M0) are 0.91, 0.74, and 0.63, respectively. The ratio of RHA flexural strength to the control samples increased with age, confirming that the flexural strength of the RHA samples continuously increased from 7 days to 28 days. The ratios increased from 0.73 at 7 days to 0.91 at 28 days for M1 (5% RHA), from 0.61 at 7 days to 0.74 at 28 days for M2 (10% RHA), and from 0.57 at 7 days to 0.63 at 28 days for M3 (20% RHA). Therefore, like compressive strength, this study predicts that the ratio of the flexural strength of the 5% RHA samples will be greater than 1.0 past 28 days. This locally sourced RHA reduced the flexural strength at 7 and 28 days, but this study predicts that it will continuously increase after 28 days. This prediction is based on the pozzolanic reaction between the RHA and  $\text{Ca}(\text{OH})_2$ . The reaction is time-dependent; it begins slowly in the early stages but increases with time depending on the porosity of the RHA, the particle size, and the water-to-cement ratio [26]. In the early days, the C-S-H gel produced from the RHA and  $\text{Ca}(\text{OH})_2$  reaction cannot compensate for the loss of Portland cement hydration, which is replaced by the RHA. However, the C-S-H gel produced from the RHA pozzolanic reaction increases with as curing time increases. Further research on the long-term strength of RHA mortar is needed.

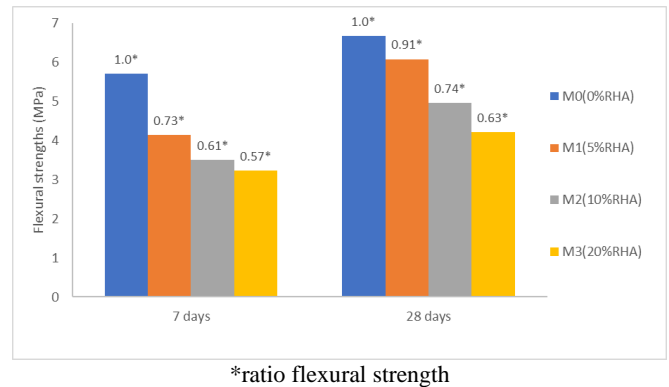


Fig. 4 Flexural strength of control and RHA blended cement mortars at 7 and 28 days

Previous research confirms that the effect of RHA on the flexural strength of mortar depends on the type of RHA, replacement proportion, and age. M. Jamil et al. investigated the effect of 10% and 20% small rice husk ash (SRHA) and large rice husk ash (LRHA) on the flexural strength of mortar at 14, 28, and 90 days [39]. They ground the RHA with steel balls to achieve two different particle sizes, which they retrieved by dry sieving. SRHA was about  $5 \pm 2\%$  by weight of the ground material retained on a 45 mm sieve, whereas LRHA was about  $34 \pm 2\%$  by weight of the ground material retained on a 45 mm sieve. Both SRHA and LRHA contributed to reducing the flexural strength at 14 days compared with the control mortar. However, at 28 and 90 days of curing, the flexural strength of the 10% SRHA and 20% SRHA mortars was higher than the control mortar. In contrast, the flexural strength of the 10% LRHA and 20% LRHA mortars was lower than the control mortar, even after 28 and 90 days of curing. The authors' results also stated that the pozzolanic and filler effects of the LRHA particles were less significant at later ages compared with the hydration effect of the control mortar. This again confirms that the particle size of the RHA influenced the flexural strength of the mortar in a similar pattern to that of compressive strength [39]. The influence of the particle size of RHA on flexural strength is also supported by other research [40, 41]. The effect of the particle size of this locally sourced RHA on flexural strength warrants further study.

### 3.4. Microstructure

SEM was used to determine the effect of RHA on the microstructure of cement mortar at both 7 days (Fig. 5a–d) and 28 days (Fig. 5e–h). Previous research reported that the  $\text{SiO}_2$  in RHA will react with  $\text{Ca}(\text{OH})_2$  to produce a C-S-H gel, which determines the strength of the mortar; further, the paste containing RHA had a lower  $\text{Ca}(\text{OH})_2$  content than the control Portland cement paste [42, 43]. The addition of RHA slowed down cement hydration at an early age, as the pozzolanic activities of the RHA paste were more substantial at later ages than at earlier ages. This is due to the porous structure of the RHA particles [44].

Water absorbed in porous RHA works as the internal curing agent, increasing the cement hydration at a later age. Therefore, the pozzolanic reaction of RHA in Portland cement depends on the porosity of the RHA.

The particle size of the RHA also determines the porosity and strength of the mortar due to the related filling effects.

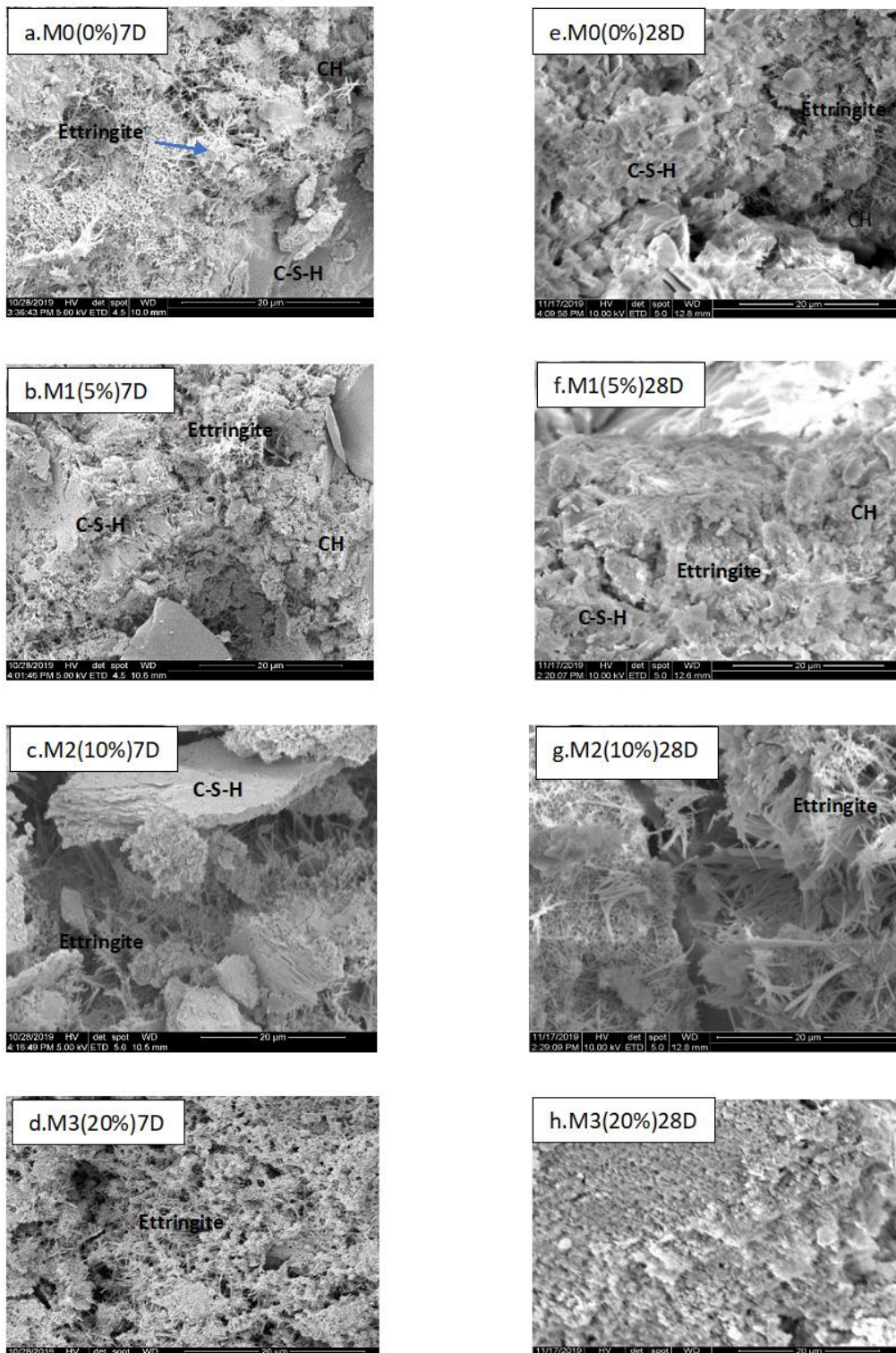


Fig. 5 SEM images of control and RHA blended cement mortars at 7 and 28 days

At 7 days, the SEM images showed that the reaction between RHA and CH was still very weak. Specifically, there was less C-S-H gel when the RHA increased, and RHA was still present in the cement paste; this mainly appeared in the 20% RHA samples. This result explains the strength reduction in the RHA samples compared with the control, as the more RHA

was added, the less Portland cement there was. This reduced the amount of C-S-H gel produced while the pozzolanic reaction between RHA and CH was still very low at this early age. At 28 days, the more pozzolanic reaction between RHA and  $\text{Ca}(\text{OH})_2$  led to more CSH gel in 28-day age samples than 7-day age samples. However, again at 28 days, the CSH gel in

RHA samples is still less than that in the control samples, and the more RHA added, the less CHS gel due to less Portland cement (replaced by RHA) while the reaction of RHA and  $\text{Ca}(\text{OH})_2$  is still low even at 28 days. However, from the SEM image, we can see that the RHA filled the gap of cement mortar paste. The less pozzolanic reaction of RHA causes the less dense of the paste and reduction in the strength of RHA blended mortar. Fig. 5a-d shows that more CH and porosity appeared on the 5% and 20% RHA blended mortar than 10% RHA blended mortar at seven days and 28 days. This is confirmed by the previous research, where the grinding of RHA has affected the microstructure of blended cement mortar in which unground rice husk ash (URHA) and ground rice husk ash (GRHA) were investigated. The URHA is coarsely graded compared to others, and the average particle sizes of URHA, GRHA are about 30  $\mu\text{m}$  and 6  $\mu\text{m}$ , respectively. Research shows that the URHA influenced the porous structure of blended mortar due to creating internal porosity within the matrix and holding available water within their internal pores. The microstructure of URHA mortar indicates a relatively lesser dense paste in a less significant pozzolanic reaction [45].

### 3.5. Porosity

The pore size distribution of the control and RHA mortars at seven days are shown in Fig. 6, while their effective porosities are given in Table 3. Fig. 6 shows the range of pore diameter in which significant levels of differential pore volume are observed and the range when the differential pore volume is at or near zero. The diameter zones showing significant differential pore volume represent porosity, while the range indicating zero differential pore volume represents a non-porous zone. Based on these criteria, it can be observed that M0(0%RHA), M1(5%RHA), M2(10%RHA), and M3(20%RHA) have a unimodal pore distribution (Fig. 6). The pore distribution is considered unimodal when a single range of pore volume is observed within the differential pore volume graphs. In contrast, a double range of pore diameters with significant differential pore volume separated by a diameter range with nearly zero differential pore volume is referred to as bimodal pore distribution [46]. The pore volume of the control mortar M0, M1(5%RHA), M2(10%RHA) and M3(20%RHA) are in the range of 0.01–1.0  $\mu\text{m}$ , 0.01–9.0  $\mu\text{m}$ ; 0.01–9.0  $\mu\text{m}$ ; and 0.01–100  $\mu\text{m}$  respectively. The control M0 and M1(5%RHA) have a high volume of their pore diameter within 0.2  $\mu\text{m}$  and 0.8  $\mu\text{m}$  with the peak differential pore volume of around 76  $\text{mm}^3/\text{g}$  and around 60  $\text{mm}^3/\text{g}$  for the control M0 and M1(5%RHA) respectively. The M2(10%RHA) has a high volume of its pore diameter within 0.4  $\mu\text{m}$  and 1.7  $\mu\text{m}$  with a peak differential pore volume of around 35  $\text{mm}^3/\text{g}$ . The M3(20%RHA) has a high volume of its pore diameter

within 16  $\mu\text{m}$  and 35  $\mu\text{m}$  with the peak differential pore volume of around 130  $\text{mm}^3/\text{g}$ . This agrees well with the strength of mortar as the high pore volume resulted in the low strength.

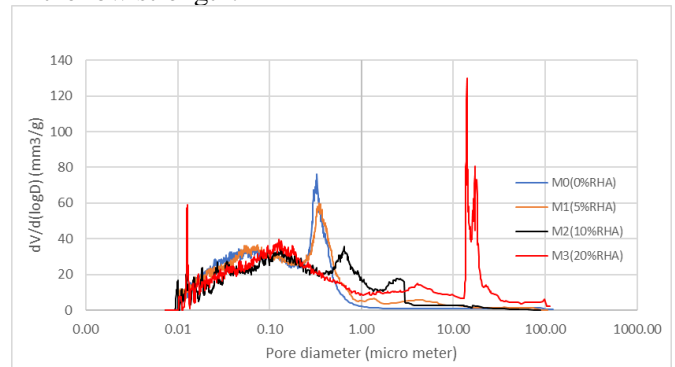


Fig. 6 Differential volume of intruded mercury versus pore diameter of mortars at seven days

Fig. 7 shows the cumulative pore volume curves of the control M0 and RHA mortar at seven days. At seven days, RHA increases the intrudable pore volume of the mortar; the intrudable pore volume of the control M0, M1 (5% RHA), M2 (10% RHA), and M3 (20% RHA) are 52.73  $\text{mm}^3/\text{g}$ , 57.22  $\text{mm}^3/\text{g}$ , 53.33  $\text{mm}^3/\text{g}$ , and 68.24  $\text{mm}^3/\text{g}$  respectively.

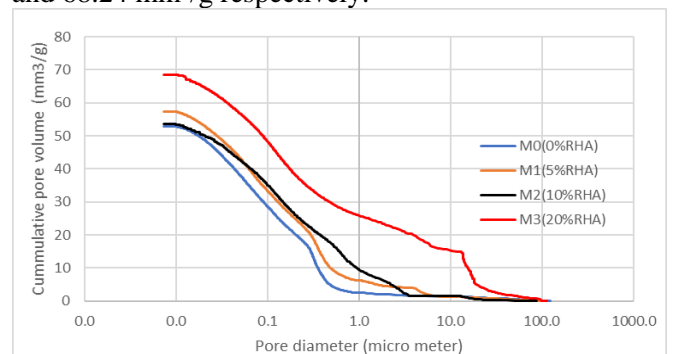


Fig. 7 Intrudable porosity for the control and RHA blended mortar at seven days

The pore size distributions of the control and RHA mortar at 28 days are shown in Fig. 8, while their effective porosities are given in Table 3. Fig. 8 shows the pore diameter range in which significant levels of differential pore volume are observed and the range where the differential pore volume is at or near zero. Again, it can be observed that M0 (0% RHA), M1 (5% RHA), M2 (10% RHA), and M3 (20% RHA) have a unimodal pore distribution (Fig. 8). The pore volumes of the control mortar M0, M1 (5% RHA), M2 (10% RHA), and M3 (20% RHA) are in the range of 0.01–1.0  $\mu\text{m}$ , 0.01–1.2  $\mu\text{m}$ , 0.01–100  $\mu\text{m}$ , and 0.01–100  $\mu\text{m}$ , respectively. The control M0 has a high volume of pore diameter within 0.3  $\mu\text{m}$  and 1.0  $\mu\text{m}$  with a peak differential pore volume of around 74  $\text{mm}^3/\text{g}$ . M1 (5% RHA) has a high volume of pore diameter within 0.01  $\mu\text{m}$  and 0.02  $\mu\text{m}$  with a peak differential pore volume of around 61  $\text{mm}^3/\text{g}$ . M2 (10% RHA) has a high volume of pore diameter within 0.06  $\mu\text{m}$  and 0.14  $\mu\text{m}$  with a peak differential pore volume of around 27  $\text{mm}^3/\text{g}$ . M3 (20% RHA) has a high volume of pore



diameter within 13  $\mu\text{m}$  and 37  $\mu\text{m}$  with a peak differential pore volume of around 96  $\text{mm}^3/\text{g}$ . This also agrees well with the strength of mortar, as the high pore volume resulted in low strength at 28 days.

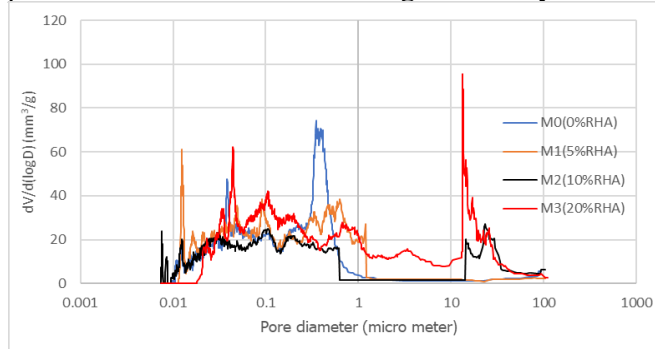


Fig. 8 Differential volume of intruded mercury versus pore diameter of mortars at 28 days

Fig. 9 shows the cumulative pore volume curves of the control M0 and RHA mortar at 28 days. At 28 days 5% RHA and 20% RHA increase the intrudable pore volume of the mortar, while 10% RHA reduces the intrudable pore volume. The intrudable pore volume of the control M0, M1(5% RHA), M2 (10% RHA), and M3 (20% RHA) are 47.43  $\text{mm}^3/\text{g}$ , 51.77  $\text{mm}^3/\text{g}$ , 41.02  $\text{mm}^3/\text{g}$ , and 70.89  $\text{mm}^3/\text{g}$ , respectively.

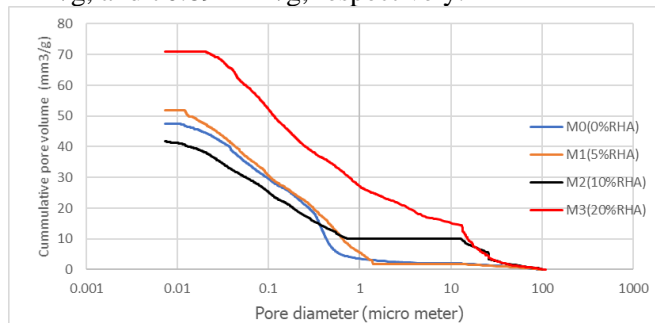


Fig. 9 Intrudable porosity for the control and RHA blended cement mortars at 28 days

Previous research investigated the porosities and pore size distribution of 10% RHA cement paste. They concluded that the pore size of all ground RHA paste decreases with increased curing time due to the pozzolanic reaction, which fills the voids between grains with their products. It is also found that finer RHA paste has less pore size distribution than others [47]. This again suggests that porosity and pore size distribution depends on RHA particle size, and further research on the effect of RHA particle size on the porosity and pore size distribution of RHA mortar should be conducted.

Table 3 shows that 5% RHA and 20% RHA increased effective porosities, while 10% RHA reduced the effective porosity at both 7 and 28 days. At 7 days, while the effective porosity of the control is 11.579%, the effective porosities of 5% RHA and 20% RHA mortar are 11.983% and 13.612%, respectively, representing increases of 3.5% and 17.6%, respectively, compared to the control samples. By contrast, the effective porosity of 10% RHA mortar is

11.301%, showing a slight reduction of 2.4% when compared with the control samples. At 28 days, while the effective porosity of the control is 10.012%, the effective porosities of 5% and 20% RHA mortar are 10.623% and 13.686%, respectively, representing an increase of 6.1% and 36.7%, respectively, compared with the control samples. By contrast, the effective porosity of 10% RHA mortar is 8.282% and shows a reduction of 17.3% compared to the control samples. Table 3 also shows that aging the samples seven to 28 days, the effective porosities of all the control, M1(5% RHA), M2(10% RHA) reduced, while sample M3 (20% RHA) remained the same. The same results were applied to the cumulative intrusion volume. The 5% RHA and 20% RHA samples showed an increase in cumulative intrusion volume, while 10% RHA reduced the cumulative intrusion volume at both seven days and 28 days and adding the aging effect that seven to 28 days had, the cumulative intrusion volume of control samples M1 (5% RHA) and M2 (10% RHA) was reduced, while sample M3 (20% RHA) remained the same. This concurs with previous research which showed that the porosity of RHA mixed concrete reduced with curing time due to an additional pozzolanic reaction [48]. Table 3 shows that locally sourced RHA from Vietnam increases porosity when 20% of the RHA was used to replace OPC while 10% RHA slightly reduced the total porosity at both seven and 28 days. This can be explained by the fact that the size of the particles of the Vietnam RHA used in this experiment were large and the filling effect did not function effectively with a replacement proportion of 20%.

Table 3 Summary of porosity data

Sample ID	Age (days)	Effective porosity (%)	Cumulative intruded volume ( $\text{mm}^3/\text{g}$ )
M0-7D	7	11.579	52.73
M1-7D	7	11.983	57.22
M2-7D	7	11.301	53.33
M3-7D	7	13.612	68.24
M0-28D	28	10.012	47.43
M1-28D	28	10.623	51.77
M2-28D	28	8.282	41.02
M3-28D	28	13.686	70.89

## 4. Conclusion

Based on the results described in this paper, the following conclusions can be made:

1. RHA reduces the workability of mortar, unless a water reducing admixture is added. The reduction in the workability of RHA blended mortar is demonstrated by the fact that the porosity of the RHA and the increase in the surface area of the RHA absorbed the water.

2. Within the range of investigation, locally sourced RHA reduced both the flexural strength and compressive strength at 28 days. This is due to the late



reaction of the RHA and  $\text{Ca}(\text{OH})_2$  and is dependent on the type of RHA. It is predicted that the strength of the RHA mortar will be higher than that of the control sample after 28 ages.

3. SEM images show that the CSH in RHA samples was still less than that of the control samples, and if more RHA was added, less CHS gel was produced as the reaction of RHA and  $\text{Ca}(\text{OH})_2$  was still low, even at 28 days. However, we can see from the SEM image that the RHA filled the gaps in the cement mortar paste.

4. Both the control samples and RHA mortar have a unimodal pore distribution. At 5% and 20% RHA, the effective porosity and cumulative intrusion volume increased, while 10% RHA reduced the effective porosity and cumulative intrusion volume at both seven days and 28 days.

5. With the effect that aging for seven to 28 days had, the cumulative intrusion volume of the control samples M1 (5% RHA) and M2 (10% RHA) was reduced, while sample M3 (20% RHA) remained the same.

6. Further research on the strength of aged RHA blended mortar needs to be conducted for the investigation of the long term pozzolanic reaction of RHA and  $\text{Ca}(\text{OH})_2$ , and the effectiveness thereof on long term strength and porosity.

7. Further research of the effect that the particle size of RHA has on the strength, porosity and pore size distribution of blended cement mortar should be investigated.

## Acknowledgments

The authors would like to express their gratitude to The University of Danang, University of Science and Technology, Vietnam, for funding and supports throughout this research.

## Funding

This work was supported by The University of Danang, University of Science and Technology, code number of Project: T2020-02-28.

## References

[1] CHATTOPADHYAY B. Genetically-Enriched Microbe-Facilitated Self-Healing Nano-Concrete. In: LIEW M. S., NGUYEN-TRI P., NGUYEN T. A., & KAKOOEI S. *Smart Nanoconcretes and Cement-Based Materials: Properties, Modelling and Applications. Micro and Nano Technologies*. Elsevier, 2020: 461-483. <https://doi.org/10.1016/B978-0-12-817854-6.00020-9>

[2] MINISTRY OF SCIENCE AND TECHNOLOGY. *TCVN 4314: 2003: Mortar for masonry – Specifications*. 2003.

[3] NOOR A. M., SALIHUDDIN R. S., and MAHYUDDIN R. Performance of high workability slag cement mortar for ferrocement. *Building and Environment*, 2007, 42(7): 2710-2717. <https://doi.org/10.1016/j.buildenv.2006.07.015>

[4] CHINDAPRASIRT P., & RUKZON S. Strength, porosity and corrosion resistance of ternary blend Portland cement, rice husk ash and fly ash mortar. *Construction and Building Materials*, 2008, 22(8): 1601–1606. <https://doi.org/10.1016/j.conbuildmat.2007.06.010>

[5] BALAKRISHNAN B., & ABDUL AWAL A.S.M. Durability properties of concrete containing high volume Malaysian fly ash. *International Journal of Research in Engineering and Technology*, 2014, 3(4): 529–533. <https://doi.org/10.15623/ijret.2014.0304093>

[6] THOMAS M. *Optimizing the use of fly ash in concrete*. n.d. [https://www.cement.org/docs/default-source/fc\\_concrete\\_technology/is548-optimizing-the-use-of-fly-ash-concrete.pdf](https://www.cement.org/docs/default-source/fc_concrete_technology/is548-optimizing-the-use-of-fly-ash-concrete.pdf)

[7] ASTM INTERNATIONAL. *ASTM C618-19: Standard Specification for Coal Fly Ash and Raw or Calcined Natural Pozzolan for Use in Concrete*. ASTM International, West Conshohocken, Pennsylvania, 2017. <https://www.astm.org/Standards/C618.htm>

[8] CANADIAN STANDARDS ASSOCIATION. *CAN/CSA A3001-03: Cementitious Materials for Use in Concrete*. Canadian Standards Association, Mississauga, 2003.

[9] NGUYEN C. V., LAMBERT P., and BUI V. N. Effect of locally sourced pozzolan on corrosion resistance of steel in reinforced concrete beams. *International Journal of Civil Engineering*, 2020, 18: 619–630. <https://doi.org/10.1007/s40999-019-00492-5>

[10] NGUYEN C. V., LAMBERT P., and TRAN Q. H. Effect of Vietnamese fly ash on selected physical properties, durability and probability of corrosion of steel in concrete. *Materials*, 2019, 12(4): 593. <https://doi.org/10.3390/ma12040593>

[11] THOMAS M., SHEHATA M., and SHASHIPRAKASH S. The use of fly ash in concrete: classification by composition. *Cement and Concrete Aggregates*, 1999, 21: 105–110. <https://doi.org/10.1520/CCA10423J>

[12] BHANUMATHIDAS N., & MEHTA P.K. Concrete mixtures made with ternary blended cements containing fly ash and rice-husk ash. Proceedings of the 7th International Conference CANMET, Chennai, 2004, pp. 379–391. <https://www.concrete.org/publications/internationalconcreteabstractsportal.aspx?m=details&i=10505>

[13] RODRIGUEZ G. S. Strength development of concrete with rice-husk ash. *Cement and Concrete Composites*, 2006, 28(2): 158–160. <https://doi.org/10.1016/j.cemconcomp.2005.09.005>

[14] RODRIGUEZ G. S., RIBEIRO A. B., and GONÇALVES A. Effects of RHA on autogenous shrinkage of Portland cement pastes. *Cement and Concrete Composites*, 2008, 30(10): 892–897. <https://doi.org/10.1016/j.cemconcomp.2008.06.014>

[15] BUI D.D. *Rice husk ash as a mineral admixture for high performance concrete*. PhD Thesis. Delft University of Technology, Delft, 2001.

[16] FOOD AND AGRICULTURE ORGANIZATION OF THE UNITED NATIONS. *FAO Rice Market Monitor (RMM)*. 2018. <http://www.fao.org/economic/est/publications/rice-publications/rice-market-monitor-rmm/vn/>

[17] NGUYEN V. T. *Rice husk ash as a mineral admixture for ultra-high performance concrete*. PhD Thesis. Delft University, Delft, 2011.

[18] ZERBINO R., GIACCIO G., and ISAIA G. C. Concrete incorporating rice-husk ash without processing.

- Construction and Building Materials*, 2011, 25(1): 371–378. <https://doi.org/10.1016/j.conbuildmat.2010.06.016>
- [19] GIVI A. N., RASHID S. A., AZIZ F. N. A., and SALLEH M. A. M. Assessment of the effects of rice husk ash particle size on strength, water permeability and workability of binary blended concrete. *Construction and Building Materials*, 2010, 24(11): 2145–2150. <https://doi.org/10.1016/j.conbuildmat.2010.04.045>
- [20] LE H. T., SIEWERT K., & LUDWIGN H. M. Synergistic effects of rice husk ash and fly ash on properties of self-compacting high performance concrete. Proceedings of the Symposium on Ultra High Performance Concrete and Nanotechnology for High Performance Construction Materials, Kassel, 2012, pp. 187–195.
- [21] NGUYEN V. T., YE G., BREUGEL K. V., FRAAIJ A. L. A., and BUI D. D. The study of using rice husk ash to produce ultra high performance concrete. *Construction and Building Materials*, 2011, 25(4): 2030–2035. <https://doi.org/10.1016/j.conbuildmat.2010.11.046>
- [22] KANTAPONG W. P., TACHAI L., and KATSUYOSHI K. Effect of Rice Husk Ash Silica as Cement Replacement for Making Construction Mortar. *Key Engineering Materials*, 2018, 775: 624–629. <https://doi.org/10.4028/www.scientific.net/KEM.775.624>
- [23] DABAI M. U., MUHAMMAD C., BAGUDO B. U., and MUSA A. Studies on the Effect of Rice Husk Ash as Cement Admixture. *Nigerian Journal of Basic and Applied Science*, 2009, 17(2): 252–256. <https://doi.org/10.4314/njbas.v17i2.49917>
- [24] BUI D. D., HU J., and STROEVEN P. Particle size effect on the strength of rice husk ash blended gap-graded Portland cement concrete. *Cement and Concrete Composites*, 2005, 27: 357–366. <https://doi.org/10.1016/j.cemconcomp.2004.05.002>
- [25] RODRIGUEZ G. S., RIBEIRO A. B., and GONÇALVES A. Effects of RHA on autogenous shrinkage of Portland cement pastes. *Cement and Concrete Composites*, 2008, 30(10): 892–897. <https://doi.org/10.1016/j.cemconcomp.2008.06.014>
- [26] CHRISTOPHER F., BOLATITO A., and AHMED S. Structure and properties of mortar and concrete with rice husk ash as partial replacement of ordinary Portland cement – A review. *International Journal of Sustainable Built and Environment*, 2017, 6(2): 675–692. <https://doi.org/10.1016/j.ijbs.2017.07.004>
- [27] ZHAO H., QI XIAO Q., HUANG D., and ZHANG S. Influence of Pore Structure on Compressive Strength of Cement Mortar. *The Scientific World Journal*, 2014, 2014: 247058. <https://doi.org/10.1155/2014/247058>
- [28] DIAMOND S. A critical comparison of mercury porosimetry and capillary condensation pore size distributions of portland cement pastes. *Cement and Concrete Research*, 1971, 1(5): 531–545. [https://doi.org/10.1016/0008-8846\(71\)90058-5](https://doi.org/10.1016/0008-8846(71)90058-5)
- [29] KJELLSSEN K. O., DETWILER R. J., and GJORV O. E. Pore structure of plain cement pastes hydrated at different temperatures. *Cement & Concrete Research*, 1990, 20: 927–933. [https://doi.org/10.1016/0008-8846\(90\)90055-3](https://doi.org/10.1016/0008-8846(90)90055-3)
- [30] MASSAZZA F. Blended cements. Special Lecture. 4th NCB International Seminar on Cement and Building Materials, New Delhi, 1994.
- [31] MINISTRY OF SCIENCE AND TECHNOLOGY. *TCVN 2682: 2009: Portland cement – Technical requirements*. 2009.
- [32] MINISTRY OF SCIENCE AND TECHNOLOGY. *TCVN 1770: 1996: Sand for construction - Technical requirements*. 1996.
- [33] AMERICAN SOCIETY FOR TESTING AND MATERIALS. *ASTM C494/C494M-19: Standard specification for chemical admixtures for concrete*. ASTM International, West Conshohocken, Pennsylvania, 2019. <https://www.astm.org/Standards/C494>
- [34] CALICA JR., M. G. Influence of Rice Husk Ash as Supplementary Material in Cement Paste and Concrete. *NLR Journal*, 2008, 2: 80–92. <http://pejard.slu.edu.ph/archives/vol2/influence-of-rice-husk-ash-as-supplementary-material-in-cement-paste-and-concrete.pdf>
- [35] KARTINI K., MAHMUD H. B., and HAMIDAH M. S. Absorption and permeability performance of Selangor rice husk ash blended grade 30 concrete. *Journal of Engineering Science and Technology*, 2010, 5(1): 1–16. [http://jestec.taylors.edu.my/Vol%205%20Issue%201%20March%2010/Vol\\_5\\_1\\_01-16\\_Kartini.pdf](http://jestec.taylors.edu.my/Vol%205%20Issue%201%20March%2010/Vol_5_1_01-16_Kartini.pdf)
- [36] MINISTRY OF SCIENCE AND TECHNOLOGY. *TCVN 3121-3:2003: Mortar for masonry - Test methods Part 3: Determination of consistence of fresh mortar (by flow table)*. 2003.
- [37] MINISTRY OF SCIENCE AND TECHNOLOGY. *TCVN 3121-11:2003: Mortar for masonry - Test methods. Part 11: Determination of flexural and compressive strength of hardened mortars*. 2003.
- [38] HWANG C. L., BUI L. A., and CHUN-TSUM C. Effect of rice husk ash on the strength and durability characteristics of concrete. *Construction and Building Materials*, 2011, 25(9): 3768–3772. <https://doi.org/10.1016/j.conbuildmat.2011.04.009>
- [39] JAMIL M., KHAN M. N. N., KARIM M. R., KAISH A. B. M. A., and ZAIN M. F. M. Physical and chemical contributions of Rice Husk Ash on the properties of mortar. *Construction and Building Materials*, 2016, 128: 185–198. <https://doi.org/10.1016/j.conbuildmat.2016.10.029>
- [40] HABEEB G. A., & FAYYADH M. M. Rice husk ash concrete: the effect of RHA average particle size on mechanical properties and drying shrinkage. *Australian Journal of Basic and Applied Sciences*, 2009, 3(3): 1616–1622. <http://www.ajbasweb.com/old/ajbas/2009/1616-1622.pdf>
- [41] ZHANG M. H., LASTRA R., and MALHOTRA V. M. Rice-husk ash paste and concrete: some aspects of hydration and the microstructure of the interfacial zone between the aggregate and paste. *Cement and Concrete Research*, 1996, 26(6): 963–977. [https://doi.org/10.1016/0008-8846\(96\)00061-0](https://doi.org/10.1016/0008-8846(96)00061-0)
- [42] YU Q., SAWAYAMA K., SUGITA S., SHOYA M., and ISOJIMA Y. The reaction between rice husk ash and Ca(OH)<sub>2</sub> solution and the nature of its product. *Cement and Concrete Research*, 1999, 29(1): 37–43. [https://doi.org/10.1016/S0008-8846\(98\)00172-0](https://doi.org/10.1016/S0008-8846(98)00172-0)
- [43] ORDONEZ L. M., PAYA J., COATS A. M., and GLASSER F. P. Reaction of Rice Husk Ash with OPC and Portlandite. *Advance in Cement Research*, 2002, 14(3): 113–119. <https://doi.org/10.1680/adcr.2002.14.3.113>
- [44] NGUYEN V. T., YE G. V., BREUGEL K., and COPUROGLU O. Hydration and microstructure of ultra high performance concrete incorporating rice husk ash. *Cement and Concrete Research*, 2011, 41(11): 1104–1111. <https://doi.org/10.1016/j.cemconres.2011.06.009>

- [45] VENKATANARAYANAN H. K., & RANGARAJU P. R. Effect of grinding of low-carbon rice husk ash on the microstructure and performance properties of blended cement concrete. *Cement and Concrete Composites*, 2015, 55: 348–363. <https://doi.org/10.1016/j.cemconcomp.2014.09.021>
- [46] PROVIS J. L., & VAN DEVENTER J. S. J. *Alkali-Activated Materials: State-of-the-Art Report*, RILEM TC 224-AAM. Springer, Dordrecht, 2014. <https://doi.org/10.1007/978-94-007-7672-2>
- [47] XU W., LO Y. T., OUYANG D., MEMON S. A., XING F., WANG W., and YUAN X. Effect of rice husk ash fineness on porosity and hydration reaction of blended cement paste. *Construction and Building Materials*, 2015, 89: 90–101. <https://doi.org/10.1016/j.conbuildmat.2015.04.030>
- [48] RUKZON S., & CHINDAPRASIRT P. Utilization of bagasse ash in high-strength concrete. *Materials & Design*, 2012, 34: 45–50. <https://doi.org/10.1016/j.matdes.2011.07.045>
- [49] ARSHAD M. F., AWANG H., JAYA R. P., ALI M. I., YUSAK M. I. M., HAININ M. R., and IBRAHIM M. H. W. Effect of Nano Black Rice Husk Ash on the Chemical and Physical Properties of Porous Concrete Pavement. *Journal of Southwest Jiaotong University*, 2018, 53(5). <http://jsju.org/index.php/journal/article/view/238>
- [50] YANGLONG Z., LIANG G., and BOWEN H. Shear Behavior of Mortar Layer in Continuous Slab Track with Different Arrangement Schemes of Embedded Steel Bars. *Journal of Southwest Jiaotong University*, 2018, 53(1). <http://jsju.org/index.php/journal/article/view/6>

#### 参考文献:

- [1] CHATTOPADHYAY B. 基因丰富的微生物促进的自修复纳米混凝土。见：LIEW M. S., NGUYEN-TRI P., NGUYEN T. A. 和 KAKOOEI S. 智能纳米混凝土和水泥基材料：性能，建模和应用。微米和纳米技术。爱思唯尔，2020：461-483. <https://doi.org/10.1016/B978-0-12-817854-6.00020-9>
- [2] 科技部。TCVN 4314：2003：砌筑砂浆—规格。2003。
- [3] NOOR A. M., SALIHUDDIN R. S. 和 MAHYUDDIN R. 高可加工性矿渣水泥砂浆的性能。建筑与环境，2007，42 (7)：2710-2717. <https://doi.org/10.1016/j.buildenv.2006.07.015>
- [4] CHINDAPRASIRT P. 和 RUKZON S. 三元掺合波特兰水泥，稻壳灰和粉煤灰砂浆的强度，孔隙率和耐腐蚀性。建筑与建材，2008，22 (8)：1601-1606. <https://doi.org/10.1016/j.conbuildmat.2007.06.010>
- [5] BALAKRISHNAN B. 和 ABDUL AWAL A.S.M. 含有大量马来西亚粉煤灰的混凝土的耐久性能。国际工程技术研究杂志，2014，3 (4)：529–533. <https://doi.org/10.15623/ijret.2014.0304093>
- [6] THOMAS M. 优化混凝土中粉煤灰的使用。n.d. [https://www.cement.org/docs/default-source/fc\\_concrete\\_technology/is548-optimizing-the-use-of-fly-ash-concrete.pdf](https://www.cement.org/docs/default-source/fc_concrete_technology/is548-optimizing-the-use-of-fly-ash-concrete.pdf)

- [7] 美国材料试验学会国际。美国材料试验学会C618-19：用于混凝土的粉煤灰和天然或煅烧天然火山灰的标准规范。美国材料试验学会国际，宾夕法尼亚州西Conshohocken，2017. <https://www.astm.org/Standards/C618.htm>
- [8] 加拿大标准协会。能够/CSA一种3001-03：用于混凝土的胶凝材料。加拿大标准协会，密西沙加，2003。
- [9] NGUYEN C. V., LAMBERT P. 和 BUI V. N. 局部来源的火山灰对钢筋混凝土梁中钢的耐腐蚀性的影响。国际土木工程杂志，2020，18：619-630. <https://doi.org/10.1007/s40999-019-00492-5>
- [10] NGUYEN C. V., LAMBERT P. 和 TRAN Q. H. 越南粉煤灰对选定的物理性能，耐久性和混凝土中钢腐蚀的可能性的影响。材料，2019，12 (4)：593. <https://doi.org/10.3390/ma12040593>
- [11] THOMAS M., SHEHATA M. 和 SHASHIPRAKASH S. 在混凝土中使用粉煤灰：按成分分类。水泥和混凝土骨料，1999，21：105-110. <https://doi.org/10.1520/CCA10423J>
- [12] BHANUMATHIDAS N. 和 MEHTA P.K. 用含粉煤灰和稻壳灰的三元混合水泥制成的混凝土混合物。第七届坎梅特国际会议论文集，2004，钦奈，第379–391页。 <https://www.concrete.org/publications/internationalconcreteabstractsportal.aspx?m=details&i=10505>
- [13] RODRIGUEZ G. S. 用稻壳灰增强混凝土强度。水泥和混凝土复合材料，2006，28 (2)：158-160. <https://doi.org/10.1016/j.cemconcomp.2005.09.005>
- [14] RODRIGUEZ G. S., RIBEIRO A. B. 和 GONÇALVES A. RHA对硅酸盐水泥浆体自生收缩的影响。水泥与混凝土复合材料，2008，30 (10)：892-897. <https://doi.org/10.1016/j.cemconcomp.2008.06.014>
- [15] BUI D.D. 稻壳灰作为高性能混凝土的矿物掺合料。博士论文。代尔夫特工业大学，代尔夫特，2001。
- [16] 联合国粮食及农业组织。粮农组织大米市场监测员。2018. <http://www.fao.org/economic/est/publications/rice-publications/rice-market-monitor-rmm/vn/>
- [17] NGUYEN V. T. 稻壳灰作为超高性能混凝土的矿物掺合料。博士论文。代尔夫特大学，代尔夫特，2011。
- [18] ZERBINO R., GIACCIO G. 和 ISAIA G. C. 掺有未经处理的稻壳灰的混凝土。建筑与建材，2011，25 (1)：371-378. <https://doi.org/10.1016/j.conbuildmat.2010.06.016>
- [19] GIVI A. N., RASHID S. A., AZIZ F. N. A. 和 SALLEH M. A. M. 评估稻壳灰粒度对二元混合混凝土的强度，透水性和可加工性的影响。建筑与建材，2010，24 (11)：2145-2150. <https://doi.org/10.1016/j.conbuildmat.2010.04.045>
- [20] LE H. T., SIEWERT K. 和 LUDWIGN H. M. 稻壳灰和粉煤灰对自密实高性能混凝土性能的协同作用

。用于高性能建筑材料的超高性能混凝土和纳米技术研讨会论文集, 卡塞尔, 2012, 第 187-195 页。

[21] NGUYEN V. T., YE G., BREUGEL K. V., FRAAIJ A. L. A. 和 BUI D. D. 使用稻壳灰生产超高性能混凝土的研究。建筑与建材, 2011, 25 (4) : 2030-

2035。 <https://doi.org/10.1016/j.conbuildmat.2010.11.046>

[22] KANTAPONG W. P., TACHAI L. 和 KATSUYOSHI K.

稻壳灰二氧化硅作为水泥替代品用于制造建筑砂浆的作用。关键工程材料, 2018, 775 : 624-

629。 <https://doi.org/10.4028/www.scientific.net/KEM.775.624>

[23] DABAI M. U., MUHAMMAD C., BAGUDO B. U. 和 MUSA A.

稻壳灰作为水泥外加剂的研究。尼日利亚基础与应用科学杂志, 2009, 17 (2) : 252-

256。 <https://doi.org/10.4314/njbas.v17i2.49917>

[24] BUI D. D., HU J. 和 STROEVEN P. 粒径对稻壳灰混合间隙分级波特兰水泥混凝土强度的影响。水泥和混凝土复合材料, 2005, 27 : 357-

366。 <https://doi.org/10.1016/j.cemconcomp.2004.05.002>

[25] RODRIGUEZ G. S., RIBEIRO A. B. 和 GONÇALVES A.

RHA对硅酸盐水泥浆体自生收缩的影响。水泥与混凝土复合材料, 2008, 30 (10) : 892-

897。 <https://doi.org/10.1016/j.cemconcomp.2008.06.014>

[26] CHRISTOPHER F., BOLATITO A. 和 AHMED S. 用稻壳灰代替普通硅酸盐水泥的砂浆和混凝土的结构和性能-

评论。国际可持续建筑与环境学报, 2017, 6 (2) : 675-

692。 <https://doi.org/10.1016/j.ijbsbe.2017.07.004>

[27] 赵华, 齐小青, 黄大和, 张胜。孔结构对水泥砂浆抗压强度的影响。科学世界杂志, 2014, 2014 : 247058

。 <https://doi.org/10.1155/2014/247058>

[28] DIAMOND S. 水银孔隙率法和硅酸盐水泥浆的毛细管冷凝孔径分布的关键比较。水泥与混凝土研究, 1971, 1 (5) : 531-

545。 [https://doi.org/10.1016/0008-8846\(71\)90058-5](https://doi.org/10.1016/0008-8846(71)90058-5)

[29] KJELLSSEN K. O., DETWILER R. J. 和 GJORV O. E. 在不同温度下水合的普通水泥浆的孔结构。水泥与混凝土研究, 1990, 20 : 927-

933。 [https://doi.org/10.1016/0008-8846\(90\)90055-3](https://doi.org/10.1016/0008-8846(90)90055-3)

[30] MASSAZZA F. 混合水泥。特别演讲。第四届国家体育局国际水泥和建筑材料研讨会, 新德里, 1994。

[31] 科技部。TCVN 2682 : 2009年 : 波特兰西门特 - 技术要求。2009。

[32] 科技部。TCVN 1770 : 1996 : 建筑用沙子- 技术要求。1996。

[33] 美国测试和材料学会。美国材料试验学会C494 / C494M-

19 : 混凝土化学外加剂的标准规范。美国材料试验学会国际, 宾夕法尼亚州西Conshohocken, 2019。

<https://www.astm.org/Standards/C494>

<https://www.astm.org/Standards/C494>

[34] CALICA JR., M. G. 稻壳灰作为辅助材料在水泥浆和混凝土中的影响。NLR 杂志, 2008, 2 : 80-92。

<http://pejard.slu.edu.ph/archives/vol2/influence-of-rice-husk-ash-as-supplementary-material-in-cement-paste-and-concrete.pdf>

[35] KARTINI K., MAHMUD H. B. 和 HAMIDAH M. S. 雪兰莪稻壳灰混合30级混凝土的吸收和渗透性能。工程科学技术学报, 2010, 5 (1) : 1-

16。 [http://jestec.taylors.edu.my/Vol%205%20Issue%201%20March%2010/Vol\\_5\\_1\\_01-16\\_Kartini.pdf](http://jestec.taylors.edu.my/Vol%205%20Issue%201%20March%2010/Vol_5_1_01-16_Kartini.pdf)

[36] 科技部。TCVN 3121-3 : 2003 : 砌体砂浆- 试验方法第3部分 : 测定新鲜砂浆的稠度 (按流表)。

2003。

[37] 科技部。TCVN 3121-11 : 2003 : 砌筑砂浆- 试验方法。第11部分 : 硬化砂浆的抗弯强度和抗压强度的测定。2003。

[38] HANG C. L., BUI L. A. 和 CHUN-TSUM C. 稻壳灰对混凝土强度和耐久性的影响。建筑与建材, 2011, 25 (9) : 3768-

3772。 <https://doi.org/10.1016/j.conbuildmat.2011.04.009>

[39] JAMIL M., KHAN M. N. N., KARIM M. R., KAISH A. B. M. A. 和 ZAIN M. F. M. 稻壳灰对砂浆性能的物理和化学贡献。建筑与建材, 2016, 128 : 185-

198。 <https://doi.org/10.1016/j.conbuildmat.2016.10.029>

[40] HABEEB G. A. 和 FAYYADH M. M. 稻壳灰混凝土 : RHA平均粒径对机械性能和干燥收缩的影响。澳大利亚基础与应用科学杂志, 2009, 3 (3) : 1616-1622。 <http://www.ajbasweb.com/old/ajbas/2009/1616-1622.pdf>

[41] ZHANG M. H., LASTRA R. 和 MALHOTRA V. M. 稻壳灰浆和混凝土 : 水化的某些方面以及集料和浆体之间的界面区域的微观结构。水泥与混凝土研究, 1996, 26 (6) : 963-977。 [https://doi.org/10.1016/0008-8846\(96\)00061-0](https://doi.org/10.1016/0008-8846(96)00061-0)

[42] YU Q., SAWAYAMA K., SUGITA S., SHOYA M. 和 ISOJIMA Y. 稻壳灰与钙 (哦) 2溶液之间的反应及其产物的性质。水泥与混凝土研究, 1999, 29 (1) : 37-

43。 [https://doi.org/10.1016/S0008-8846\(98\)00172-0](https://doi.org/10.1016/S0008-8846(98)00172-0)

[43] ORDONEZ L. M., PAYA J., COATS A. M. 和 GLASSER F. P. 稻壳灰与OPC和硅酸盐的反应。水泥研究进展, 2002, 14 (3) : 113-

119。 <https://doi.org/10.1680/adcr.2002.14.3.113>

[44] NGUYEN V. T., YE G. V., BREUGEL K. 和 COPUROGLU O. 掺入稻壳灰的超高性能混凝土的水化和微观结构。水泥与混凝土研究, 2011, 41 (11) : 1104-

1111。 <https://doi.org/10.1016/j.cemconres.2011.06.009>

[45] VENKATANARAYANYAN H. K. 和 RANGARAJU P. R. 研磨低碳稻壳灰对混合水泥混凝土的微观结构和性能的影响。水泥和混凝土复合材料, 2015, 55 : 348-

363。 <https://doi.org/10.1016/j.cemconcomp.2014.09.021>



- 
- [46] PROVIS J. L. 和 VAN DEVENTER J. S. J. 碱活化材料：最新报告，力力TC 224-美国汽车协会。施普林格，多德雷赫特，2014。  
<https://doi.org/10.1007/978-94-007-7672-2>
- [47]徐文华，罗玉堂，欧阳四，孟蒙，邢发，王文，袁X。稻壳灰细度对水泥浆掺量孔隙度和水化反应的影响。建筑与建材，2015，89：90-101。  
<https://doi.org/10.1016/j.conbuildmat.2015.04.030>
- [48] RUKZON S. 和 CHINDAPRASIRT P. 在高强度混凝土中利用蔗渣灰。材料与设计，2012，34：45-50。  
<https://doi.org/10.1016/j.matdes.2011.07.045>
- [49] ARSHAD M. F., AWANG H., JAYA R. P., ALI M. I., YUSAK M. I. M., HAININ M. R. 和 IBRAHIM M. H. W. 纳米黑米稻壳灰对多孔混凝土路面化学性质和物理性质的影响。西南交通大学学报，2018，53（5）。  
<http://jsju.org/index.php/journal/article/view/238>
- [50] YANGLONG Z., LIANG G. 和 BOWEN H. 带有不同排列方案的嵌入式钢筋在连续平板轨道上砂浆层的剪切行为。西南交通大学学报，2018，53（1）。  
<http://jsju.org/index.php/journal/article/view/6>